

Water versus Acetonitrile Coordination to Uranyl. Density Functional Study of Cooperative Polarization Effects in Solution

Michael Bühl,^{*,†} Nicolas Sieffert,[†] Alain Chaumont,[‡] and Georges Wipff[‡]

[†]School of Chemistry, University of St. Andrews, North Haugh, St. Andrews, Fife KY16 9ST, U.K., and [‡]UMR 7177 CNRS, Laboratoire MSM, Institut de Chimie, 4 rue Blaise Pascal, 67000 Strasbourg, France

Received September 23, 2010

Optimizations at the BLYP and B3LYP levels are reported for mixed uranyl-water/acetonitrile complexes $[\text{UO}_2(\text{H}_2\text{O})_{5-n}(\text{MeCN})_n]^{2+}$ ($n = 0-5$), in both the gas phase and a polarizable continuum modeling acetonitrile. Car–Parrinello molecular dynamics (CPMD) simulations have been performed for these complexes in the gas phase, and for selected species ($n = 0, 1, 3, 5$) in a periodic box of liquid acetonitrile. According to structural and energetic data, uranyl has a higher affinity for acetonitrile than for water in the gas phase, in keeping with the higher dipole moment and polarizability of acetonitrile. In acetonitrile solution, however, water is the better ligand because of specific solvation effects. Analysis of the dipole moment of the coordinated water molecule in $[\text{UO}_2(\text{H}_2\text{O})(\text{MeCN})_4]^{2+}$ reveals that the interaction with the second-shell solvent molecules (through fairly strong and persistent O–H···N hydrogen bonds) causes a significant increase of this dipole moment (by more than 1 D). This cooperative polarization of water reinforces the uranyl-water bond as well as the water solvation via strengthened $(\text{UO}_2)\text{OH}_2\cdots\text{NCMe}$ hydrogen bonds. Such cooperativity is essentially absent in the acetonitrile ligands that make much weaker $(\text{UO}_2)\text{NCMe}\cdots\text{NCMe}$ hydrogen bonds. Beyond the uranyl case, this study points to the importance of cooperative polarization effects to enhance the M^{n+} ion affinity for water in condensed phases involving $\text{M}^{n+}-\text{OH}_2\cdots\text{A}$ fragments, where A is a H-bond proton acceptor and M^{n+} is a hard cation.

1. Introduction

The use of non-aqueous solvents has enriched our knowledge of uranium chemistry tremendously. The choice of proper solvents has been instrumental, for instance, for accessing a plethora of pentavalent uranium compounds¹ or for exploring the blossoming field of organouranium chemistry.² While a lot is known about structures and speciation of uranyl complexes in aqueous solution, the extent to which this knowledge can be transferred to organic solvents is not at all obvious. Coordination chemistry of uranyl in the latter environments can also be used as a reference for studying solutions in ionic liquids,³ where unusual coordination modes can be observed.⁴ Exploration of the non-aqueous solution chemistry of uranyl complexes is thus a research area of current interest. Recent examples comprise extended

X-ray absorption fine structure (EXAFS) studies of chloride complexation to uranyl(VI) in acetonitrile⁵ or of uranyl(V) complexes in dimethylsulfoxide (DMSO).⁶

One problem encountered in these studies is that the solutions can still contain substantial amounts of water. This can be present in particular if hydrated salts are used as uranium source. In addition, it may be difficult to strictly exclude all traces of water if the solvent is hygroscopic. One key question is, what is the preferred ligand for uranyl if both water and another solvent are present simultaneously? EXAFS results have been interpreted in terms of a higher affinity of UO_2^{2+} toward water than toward acetonitrile in solution.⁵ Because the latter is frequently a stronger donor in metal complexes than the former, this result appears to be quite unexpected and worthy of a complementary computational investigation.

Many useful insights into structures and intrinsic stabilities of actinide complexes can be gained from quantum-chemical calculations, be it through ab initio wave function theory or

*To whom correspondence should be addressed. Fax: (+44)(0)1334 463808. E-mail: buehl@st-andrews.ac.uk.

(1) Arnold, P. L.; Love, J. B.; Patel, D. *Coord. Chem. Rev.* **2009**, 253, 1973–1978.

(2) See, for example, (a) Cantat, T.; Graves, C. R.; Scott, B. L.; Kiplinger, J. L. *Angew. Chem., Int. Ed.* **2009**, 48, 3681–3684. (b) Andrea, T.; Eisen, M. S. *Chem. Soc. Rev.* **2008**, 37, 550–567.

(3) Review: Billard, I.; Gaillard, C. *Radiochim. Acta* **2009**, 97, 355–359.

(4) For example, a trinitrate complex, which is unknown in water: Servaes, K.; Hennig, C.; Billard, I.; Gaillard, C.; Binnemans, K.; Gorrler-Walrand, C.; Van Deun, R. *Eur. J. Inorg. Chem.* **2007**, 5120–5126.

(5) Hennig, C.; Servaes, K.; Nockemann, P.; Van Hecke, K.; Van Meervelt, L.; Wouters, J.; Fluyt, L.; Gorrler-Walrand, C.; Van Deun, R. *Inorg. Chem.* **2008**, 47, 2987–2993.

(6) Takao, K.; Tsushima, S.; Takao, S.; Scheinost, A. C.; Bernhard, G.; Ikeda, Y.; Hennig, C. *Inorg. Chem.* **2009**, 48, 9602–9604.

density functional theory (DFT).⁷ As for the latter, hybrid DFT and small-core relativistic effective core potentials (ECPs) or all-electron relativistic treatments such as the zeroth-order regular approximation have proven fairly robust in describing the thermochemistry of actinides.^{8,9} However, one key point is still a challenge for computational uranyl chemistry, namely, solvation. This is because the species involved are often highly charged and many of the solvents are of high polarity and/or hydrogen bonding capability. Especially the latter interactions are difficult to describe with a simple polarizable continuum model (PCM), the most popular means to account for solvation in conventional, static computations.

An alternative technique to study solvation is through classical molecular dynamics (MD) simulations with explicit solvent, using either empirical or DFT-derived potentials. We have pioneered the application of both these techniques to a diverse set of uranyl complexes.^{10,11} Fully classical MD studies have since then shed light on the surfactant behavior of uranyl complexes at interfaces between immiscible liquids,¹² including systems as complex as humid ionic liquids.^{12a,c} More recently, we and others have used DFT-based Car–Parrinello molecular dynamics (CPMD) simulations to study structure, speciation, and ligand exchange reactions of uranyl(VI) complexes in aqueous solution.^{11,13} Using the BLYP functional and pointwise thermodynamic integration (PTI), a variety of thermodynamic and kinetic parameters have been reproduced reasonably well, in most cases with an accuracy of about ± 2.5 kcal/mol.^{14–16}

We now apply both static and dynamic DFT methods to address the relative binding strength of water and acetonitrile toward uranyl, studying mixed uranyl-water/acetonitrile complexes $[\text{UO}_2(\text{H}_2\text{O})_{5-n}(\text{MeCN})_n]^{2+}$ ($n = 0–5$) in the gas phase and in solution. In a recent DFT study of this competition in the gas phase it was shown that nitrile addition is favored over the addition of water ligands.¹⁷ We now present evidence that solvation reverses the relative affinities, which can be traced back to an increased polarization of the water

ligand by the second solvation shell. In a wider sense, this cooperative polarization of metal-coordinated water ligands may contribute to the fact that water is such a strong ligand competitor to hard cations, that is, that UO_2^{2+} or Ln^{3+} coordinate water if present, rather than counteranions.¹⁸

2. Computational Details

The same methods and basis sets as in our previous studies of uranyl halides were employed.^{15b,c} Non-periodic geometry optimizations were performed in the gas phase using the BLYP¹⁹ functional, the small-core Stuttgart–Dresden relativistic ECP together with its valence basis set on U²⁰ (from which the most diffuse s-, p-, d-, and f-functions were omitted each, affording a [7s6p5d3f] contraction),²¹ standard 6-31G-(d,p) basis for all other elements, and a fine integration grid (75 radial shells with 302 angular points per shell), denoted SDD. The minimum character of each stationary point was verified by computation of the harmonic vibrational frequencies, which were all real. The geometries were reoptimized with the same methods and basis sets using the PCM implementation of Tomasi and co-workers²² (employing the united-atom UFF radii and the parameters of acetonitrile), denoted PCM. Refined single-point energies were evaluated both in the gas-phase and in the continuum at the BLYP/SDD(+) level, that is, using the geometries optimized in the respective medium, the same SDD ECP and valence basis on U, and 6-311+G(d,p) basis on all other elements.²³ Estimates for the basis-set superposition error (BSSE) of individual bonds were computed for complex **1** (Scheme 1) using the Counterpoise method,²⁴ employing SDD(+) basis and the SDD geometries optimized in the respective medium. These corrections are summarized in the Supporting Information, Table S4.

The BLYP functional was chosen for direct comparison with the CPMD simulations (see below), which employed it for compatibility with our previous simulations of aqueous solutions,^{11,14–16} where this functional performs better than most other standard GGAs for describing the properties of liquid water.²⁵ Additional optimizations were performed using the B3LYP^{26,19b} functional, the same SDD ECP and valence basis on U, and cc-pVTZ basis²⁷ for all other elements (denoted pVTZ). BLYP/pVTZ and B3LYP/pVTZ single-point calculations were

(7) For some selected reviews, see: (a) Denning, R. G. *J. Phys. Chem. A* **2007**, *111*, 4125–4143. (b) Vallet, V.; Maccac, P.; Wahlgren, U.; Grenthe, I. *Theor. Chem. Acc.* **2006**, *115*, 145–160. (c) Szabó, Z.; Toraishi, T.; Vallet, V.; Grenthe, I. *Coord. Chem. Rev.* **2006**, *250*, 784–815. (d) Kaltsoyannis, N.; Hay, P. J.; Li, J.; Blaudeau, J. P.; Bursten, B. E. In *The Chemistry of the Actinide and Transactinide Elements*, 3rd ed.; Morss, L. R., Edelstein, N. M., Fuger, J., Katz, J. J., Eds.; Springer: Dordrecht, The Netherlands, 2006; Vol. 3, pp 1893–2012.

(8) Schreckenbach, G.; Shamov, G. A. *Acc. Chem. Res.* **2010**, *43*, 19–29.
(9) See, for example, Shamov, G. A.; Schreckenbach, G.; Vo, T. N. *Chem.—Eur. J.* **2007**, *13*, 4932–4947.

(10) Guilbaud, P.; Wipff, G. *J. Phys. Chem.* **1993**, *97*, 5685–5692.

(11) First CPMD studies of aqueous uranyl hydrate and nitrate: (a) Bühl, M.; Diss, R.; Wipff, G. *J. Am. Chem. Soc.* **2005**, *127*, 13506–13507. (b) Bühl, M.; Kabrede, H.; Diss, R.; Wipff, G. *J. Am. Chem. Soc.* **2006**, *128*, 6357–6368.

(12) For example, (a) Chaumont, A.; Wipff, G. *Inorg. Chem.* **2004**, *43*, 5891–5901. (b) Schurhammer, R.; Wipff, G. *J. Phys. Chem. A* **2005**, *109*, 5208–5216. (c) Chaumont, A.; Wipff, G. *Phys. Chem. Chem. Phys.* **2006**, *8*, 494–502.

(13) Nichols, P.; Bylaska, E. J.; Schenter, G. K.; de Jong, W. *J. Chem. Phys.* **2008**, *128*, 124507.

(14) Acidity constant of uranyl hydrate: Bühl, M.; Kabrede, H. *ChemPhysChem* **2006**, *7*, 2290–2293.

(15) Binding energies of nitrate and halides: (a) Bühl, M.; Golubnychiy, V. *Inorg. Chem.* **2007**, *46*, 8129–8131. (b) Bühl, M.; Sieffert, N.; Golubnychiy, V.; Wipff, G. *J. Phys. Chem. A* **2008**, *112*, 2428–2436. (c) Bühl, M.; Sieffert, N.; Wipff, G. *Chem. Phys. Lett.* **2009**, *467*, 287–293.

(16) Barrier for water exchange: (a) Bühl, M.; Kabrede, H. *Inorg. Chem.* **2006**, *45*, 3834–3836; barrier for “yl-exchange”. (b) Bühl, M.; Schreckenbach, G. *Inorg. Chem.* **2010**, *49*, 3821–3827.

(17) Schoendorff, G.; de Jong, W. A.; Gordon, M. S.; Windus, T. L. *J. Phys. Chem. A* **2010**, *114*, 8902–8912.

(18) For example, zwitterionic carboxyl ligands remain coordinated to uranyl in acetonitrile, but not in water: Nockemann, P.; Van Deun, R.; Thijs, B.; Huys, D.; Vanecht, E.; Van Hecke, K.; Van Meervelt, L.; Binnemans, K. *Inorg. Chem.* **2010**, *49*, 3351–3360.

(19) (a) Becke, A. D. *Phys. Rev. A* **1988**, *38*, 3098–3100. (b) Lee, C.; Yang, W.; Parr, R. G. *Phys. Rev. B* **1988**, *37*, 785–789.

(20) (a) Küchle, W.; Dolg, M.; Stoll, H.; Preuss, H. *J. Chem. Phys.* **1994**, *100*, 7535. (b) see the Supporting Information for details of the valence basis set used.

(21) This small-core ECP has been shown to reproduce all-electron scalar relativistic results very well, see: Odoh, S. O.; Schreckenbach, G. *J. Phys. Chem. A* **2010**, *114*, 1957–1963.

(22) As implemented in Gaussian 03: (a) Barone, V.; Cossi, M.; Tomasi, J. *J. Comput. Chem.* **1998**, *19*, 404–417. (b) Cossi, M.; Scalmani, G.; Rega, N.; Barone, V. *J. Chem. Phys.* **2002**, *117*, 43–54. (c) Cossi, M.; Crescenzi, O. *J. Chem. Phys.* **2003**, *119*, 8863–8872.

(23) (a) Krishnan, R.; Binkley, J. S.; Seeger, R.; Pople, J. A. *J. Chem. Phys.* **1980**, *72*, 650–654. (b) Clark, T.; Chandrasekhar, J.; Spitznagel, G. W.; Schleyer, P. v. R. *J. Comput. Chem.* **1983**, *4*, 294–301.

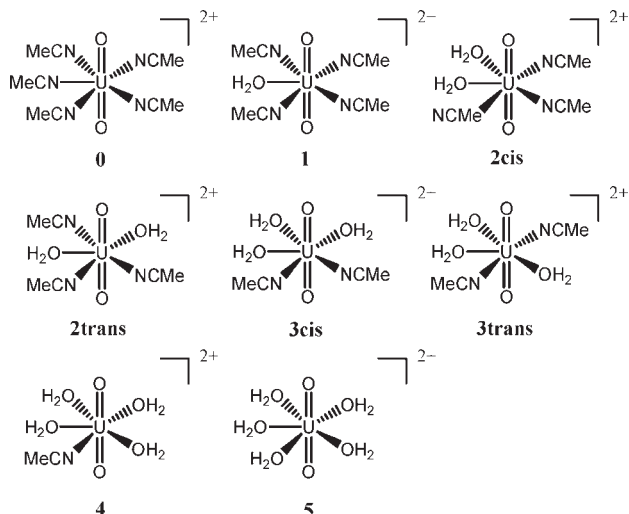
(24) Boys, S. F.; Bernardi, F. *Mol. Phys.* **1970**, *19*, 553.

(25) The initial CPMD/BLYP simulations in the Parrinello group have afforded good descriptions of liquid water, see for instance: (a) Sprik, M.; Hutter, J.; Parrinello, M. *J. Chem. Phys.* **1996**, *105*, 1142–1152, although potential shortcomings of this functional are now better appreciated, see: (b) Van deVondele, J.; Mohamed, F.; Krack, M.; Hutter, J.; Sprik, M.; Parrinello, M. *J. Chem. Phys.* **2005**, *122*, 014515, and references cited therein.

(26) Becke, A. D. *J. Chem. Phys.* **1993**, *98*, 5648–5642.

(27) (a) Dunning, T. H., Jr. *J. Chem. Phys.* **1989**, *90*, 1007–1023. (b) Kendall, R. A.; Dunning, T. H., Jr.; Harrison, R. A. *J. Chem. Phys.* **1992**, *96*, 6769–6806.

Scheme 1. Investigated Penta-Coordinated Complexes, Labeled According to the Number of Coordinated Water Molecules (0–5)



performed using these B3LYP/pVTZ geometries and the PCM approach employing the parameters of acetonitrile. Selected atomic charges were obtained from Mulliken and natural population analysis.²⁸ These calculations were performed with the Gaussian 03²⁹ suite of programs.

CPMD³⁰ simulations were performed using the BLYP functional and norm-conserving pseudopotentials that had been generated according to the Troullier and Martins procedure³¹ and transformed into the Kleinman–Bylander form.³² For uranium, the semicore (or small-core) pseudopotential was employed that had been generated and validated in ref 11. Periodic boundary conditions were imposed using cubic supercells with a lattice constant of 15 Å. Kohn–Sham orbitals were expanded in plane waves at the Γ -point up to a kinetic energy cutoff of 80 Ry. Simulations were performed in the NVT ensemble using a single Nosé–Hoover thermostat set to 320 K (frequency 1800 cm⁻¹), a fictitious electronic mass of 600 au, and a time step of 0.121 fs. To maintain the time step, hydrogen was substituted with deuterium. The somewhat higher temperature was chosen to increase solvent mobility and improve the sampling. For the solutions, the boxes contained the UO₂ moiety with the necessary number of coordinated water molecules, as well as a total of 36 acetonitrile molecules (38 for the simulation of [UO₂(H₂O)(MeCN)₅]²⁺). Long-range electrostatic interactions were treated with the Ewald method. Simulations of solutions started from pre-equilibrated classical MD snapshots using the AMBER force field³³ (200 ps with frozen solute) and were continued for 3 ps in each case; data were collected for analysis during the last picosecond.

For **5** in acetonitrile, a modified pre-equilibration procedure was trialed in addition, in which the charges on the water atoms in the AMBER force field were set to zero (to avoid a potential bias due to overstructuring). Only minor effects on structural parameters were noted (see Results

section and Supporting Information, Figure S4a). For complex **0** in solution, the simulation was continued for another 3.5 ps to ensure convergence of the observables sampled (see Supporting Information, Table S3). For the simulations of gaseous and solvated six-coordinated complexes, [UO₂(H₂O)₃(MeCN)₃]²⁺ and [UO₂(H₂O)(MeCN)₅]²⁺, additional pre-equilibration CPMD runs were performed using constraints to maintain the six-coordination and to avoid bias due to a particular starting configuration. These constraints and the resulting mean forces on them are detailed in Supporting Information, Tables S1 and S2. After dissociation of one MeCN ligand from these systems, the simulations were prolonged and taken as those of **3** and **1**, respectively.

Selected geometries were optimized in the gas phase using the same setup as described above until the maximum gradient was less than 5×10^{-4} a.u. (denoted CP-opt). The resulting charge distributions were analyzed by transforming the Kohn–Sham MOs into maximally localized Wannier functions characterized by their centers.³⁴ For dynamic ensembles, Wannier centers were evaluated for 50 snapshots taken during the last picosecond. Statistical analysis of this data is presented in Supporting Information, Table S6 and Figure S7. All CP-opt computations and CPMD simulations were performed with the CPMD program.³⁵

3. Results

3.1. Structures. The structures of the complexes investigated in this study are displayed in Scheme 1. Geometries have been optimized in the gas phase and in a polarizable continuum (PCM) modeling bulk acetonitrile. Geometric parameters are collected in Table 1. According to preliminary calculations for **2** and **3** at the B3LYP level, the trans isomers are slightly more stable than the cis forms (by ca. 0.5 to 0.6 kcal/mol). Thus, only the data for the former are given.

In addition, CPMD simulations have been performed both in the gas phase and in acetonitrile solution. Essentially the same methods have been used as in our previous studies on uranyl complexes in aqueous solution,^{11,14–16} except for a larger box. Going from small, mobile solvent molecules like water to larger, more sluggish rods like acetonitrile raises concerns about equilibration and solvent mobility on the short time scales accessible with CPMD. Documentation of the liquid-like character of the simulated solutions (radial distribution functions, acetonitrile diffusion coefficient) and convergence of the geometrical parameters with simulation time is provided in the Supporting Information, Figures S2–S5 and Table S6.

The U–O_{eq} distances to the water ligands decrease considerably on going from the gas phase to the bulk, by up to 0.1 Å for static minima and a PCM model (compare, for example, BLYP Gas and BLYP PCM data in Table 1), and by up to 0.15 Å for dynamic ensembles with explicit solvation (compare CPMD Gas and CPMD Solution data in Table 1). This finding contrasts with that for the

(28) Reed, A. E.; Curtiss, L. A.; Weinhold, F. *Chem. Rev.* **1988**, *88*, 899–926.

(29) Frisch, M. J.; Pople, J. A. et al. *Gaussian 03*, Revision E.01; Gaussian, Inc.: Pittsburgh, PA, 2003.

(30) Car, R.; Parrinello, M. *Phys. Rev. Lett.* **1985**, *55*, 2471–2474.

(31) Troullier, N.; Martins, J. L. *Phys. Rev. B* **1991**, *43*, 1993–2006.

(32) Kleinman, L.; Bylander, D. M. *Phys. Rev. Lett.* **1982**, *48*, 1425–1428.

(33) Case, D. A.; Pearlman, D. A.; Caldwell, J. W.; Cheatham, T. E., III; Wang, J.; Ross, W. S.; Simmerling, C. L.; Darden, T. A.; Merz, K. M.; Stanton, R. V.; Cheng, A. L.; Vincent, J. J.; Crowley, M.; Tsui, V.; Gohlke, H.; Radmer, R. J.; Duan, Y.; Pitera, J.; Massova, I.; Seibel, G. L.; Singh, U. C.; Weiner, P. K.; Kollman, P. A. *AMBER7*, 7; University of California: San Francisco, CA, 2002.

(34) (a) Marzari, N.; Vanderbilt, D. *Phys. Rev. B* **1997**, *56*, 12847.

(b) Silvestrelli, P. L.; Marzari, N.; Vanderbilt, D.; Parrinello, M. *Solid State Commun.* **1998**, *107*, 7; Wannier functions are a generalization to infinite periodic systems of the Boys localized orbitals [(c) Boys, S. F. In *Quantum Theory of Atoms, Molecules, and the Solid State*; Löwdin, P.-O., Ed.; Academic Press: New York, 1966; p 253]. Wannier centers are the maxima of these localized orbitals denoting the highest negative charge concentration. For a review with some more background on Wannier functions and centers see: (d) Tse, J. S. *Annu. Rev. Phys. Chem.* **2002**, *53*, 249–290.

(35) CPMD, Version 3.13.1; Copyright IBM Corp. 1990–2008, Copyright MPI für Festkörperforschung, Stuttgart, Germany, 1997–2001.

Table 1. Mean Optimized or Simulated U–X Distances (in Å; X = O_{ax}, N, or O_{eq}), Evaluated in the Gas Phase, a Polarizable Continuum, or an Explicit Acetonitrile Solution

complex	<i>r</i> , Å	B3LYP ^a	BLYP ^b	BLYP ^b	CP-opt	CPMD ^d	CPMD ^d	exp ^e
		gas	gas	PCM ^c	gas	gas	solution	
0	U–O _{ax}	1.74	1.78	1.79	1.78	1.78(2)	1.80 (4)	1.77(2)
	U–N	2.55	2.55	2.53	2.55	2.57(6)	2.55 (10)	2.53(2)
1	U–O _{ax}	1.75	1.79	1.79	1.78	1.78(1)	1.80(2) ^f	
	U–N	2.55	2.55	2.54	2.54	2.58(10)	2.55(10) ^f	
1·2MeCN ^g	U–O _{eq}	2.51	2.49	2.39	2.51	2.55(8)	2.40(7) ^f	
	U–O _{ax}		1.79		1.79	1.79(1)		
	U–N		2.59		2.57	2.61(10)		
2 trans	U–O _{eq}		2.32		2.36	2.38(7)		
	U–O _{ax}	1.75	1.78	1.79	1.78	1.78(1)		
	U–N	2.54	2.55	2.55	2.54	2.58(10)		
3 trans	U–O _{eq}	2.50	2.49	2.40	2.50	2.54(7)		
	U–O _{ax}	1.75	1.78	1.80	1.78	1.79(3)	1.80(4) ^h	
	U–N	2.53	2.55	2.56	2.54	2.55(9)	2.59(11) ^h	
4	U–O _{eq}	2.50	2.50	2.42	2.50	2.55(10)	2.44(9) ^h	
	U–O _{ax}	1.75	1.78	1.80	1.78	1.78(2)		
	U–N	2.52	2.53	2.58	2.51	2.55(9)		
5	U–O _{eq}	2.50	2.50	2.45	2.51	2.54(9)		
	U–O _{ax}	1.74	1.78 ⁱ	1.80	1.78	1.78(1) ⁱ	1.81(4) ^k	1.76(2)
	U–O _{eq}	2.50	2.50 ⁱ	2.46	2.50	2.54(8) ⁱ	2.47(9) ^k	2.43(2)

^a B3LYP/pVTZ level. ^b BLYP/SDD level. ^c PCM using parameters of acetonitrile. ^d Averages over the last picosecond of MD, with fluctuations given in parentheses (standard deviations). ^e EXAFS data from ref 5 (value for **0** given as “extrapolation to the hypothetical limiting complex”). ^f Complex obtained after the spontaneous dissociation of one MeCN ligand from [UO₂(H₂O)(MeCN)₅]²⁺ in solution. ^g Microsolvated complex **1A**, that is, with two second-shell MeCN molecules hydrogen-bonded to the aquo ligand (see Figures 2b and 3 for a representative structure). ^h Complex obtained after the spontaneous dissociation of one MeCN ligand from [UO₂(H₂O)₃(MeCN)₃]²⁺ in solution. ⁱ From ref 11a (box length 11.5 Å). ^k Similar values (1.80(4) Å and 2.49(10) Å) are obtained with a different pre-equilibration procedure (see Computational Details).

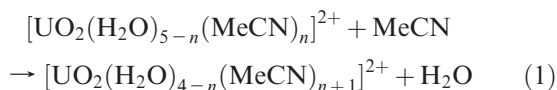
Table 2. Reaction Energies for the Successive Displacement of One Aquo Ligand with Acetonitrile According to Equation 1 (in kcal/mol)

<i>n</i>	B3LYP/pVTZ		BLYP/SDD(+)		BLYP BSSE corrected ^a	
	Δ <i>E</i> _{gas}	Δ <i>E</i> _{PCM}	Δ <i>E</i> _{gas}	Δ <i>E</i> _{PCM}	Δ <i>E</i> _{gas} ^{CP}	Δ <i>E</i> _{PCM} ^{CP}
0	−12.4	4.8	−13.2	2.2	−14.4	1.0
1	−11.0	4.1	−12.0	2.1	−13.2	0.9
2	−9.2	5.3	−10.2	3.4	−11.4	2.2
3	−7.6	5.7	−8.5	4.4	−9.7	3.2
4	−6.6	5.9	−7.5	4.8	−8.7	3.6

^a Including Counterpoise correction for BSSE (Δ*E*^{CP} = Δ*E* + δ*E*_{BSSE}, with δ*E*_{BSSE} = (0.7 to 1.9) kcal/mol). See Computational Details and Supporting Information, Table S4.

U–N bond distances, which are rather similar for all complexes and are less sensitive to solvation: most optimized or MD-averaged bond lengths are between 2.53 and 2.58 Å, irrespective whether in the gas phase, a polarizable continuum, or in an explicit solution (BLYP level, Table 1). Only occasionally a slightly longer mean distance is found during CPMD. It is interesting to note, however, that the small changes in the U–N bond distances upon solvation, are systematic: the more water ligands are present, the longer the U–N distances become in the solvent (compare, for instance the CPMD Solution results for **1** and **3 trans**). Thus, as the complex is immersed in solution, it appears that U–O bonds are strengthened while U–N bonds are little affected or slightly weakened.

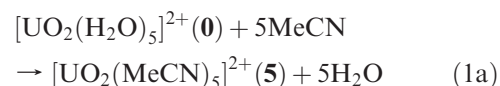
3.2. Energetics. The relative stability of water versus acetonitrile complexes is assessed via energies for successive ligand displacement reactions according to:



The results are summarized in Table 2. In terms of single point energies in the continuum, B3LYP/pVTZ

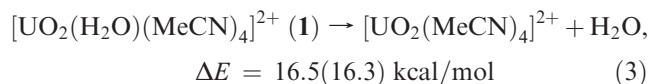
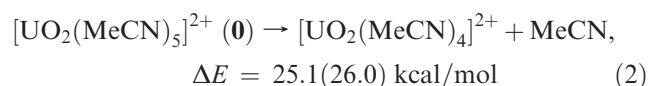
and BLYP/pVTZ results (not shown) are very similar. The quantitative numbers depend somewhat on the density functional and the treatment of BSSE, but the qualitative conclusion is independent of these technical issues: All Δ*E*_{gas} values are negative, all Δ*E*_{PCM} values are positive. Thus, acetonitrile is indicated to be a better ligand than water in the gas phase, whereas it is the other way round in solution.

The cumulative sums over *n* = 0 to 4, that is, the driving forces for the overall reaction



is considerable, for example, Δ*E*_{gas} and Δ*E*_{PCM} of −51.4 kcal/mol and +17.0 kcal/mol, respectively, at the BLYP/SDD(+) level. By far the largest contribution to this difference stems from the electrostatic interaction between polarized solute and continuum, which at the same level amount to about −211 kcal/mol and −121 kcal/mol for **0** and **5**, respectively.

3.3. Molecular Dynamics Simulations. To gain further insights into the relative binding strengths of the two ligands, we have performed additional CPMD simulations. Further validation of the methodology used (pseudopotential, plane-wave cutoff) is provided by the absolute gas-phase binding energies in the prototypical complexes **0** and **1** at the BLYP/SDD level (BLYP/CP-opt in parentheses):



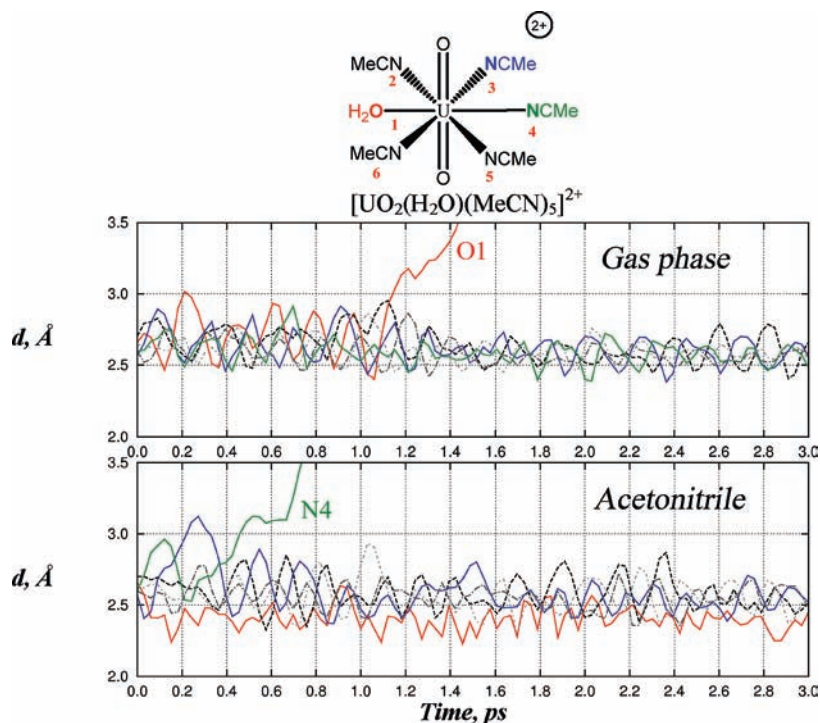


Figure 1. Time-evolution of U–X distances (in Å, X = O_{H₂O} or N_{MeCN}) for the six equatorial ligands of [UO₂(H₂O)(MeCN)₅]²⁺ in the gas phase (top) and in acetonitrile solution (bottom). Colors: O1, red; N3, blue; N4, green; N2, N5, and N6, gray.

The stronger affinity of the tetrakis(acetonitrile)-uranyl fragment toward MeCN than toward H₂O in the gas phase is clearly apparent from these data, and the near-quantitative agreement between the two types of calculations with their different setup (isolated systems with Gaussian basis sets versus periodic supercells with plane-wave basis) is very reassuring.

Relative acetonitrile versus water affinities have been further assessed in “computer experiments” in the dynamical ensemble starting from mixed six-coordinate complexes. These are models for intermediates (or transition states) involved in ligand exchange reactions following an associative (A) or associative interchange (I_A) mechanism (cf. the related hexaquo complex studied in reference 16a).³⁶ After pre-equilibration with suitable constraints, [UO₂(H₂O)₃(MeCN)₃]²⁺ immediately (within 0.2 ps) lost a water ligand in the gas phase, but an acetonitrile ligand in solution (see Supporting Information, Figure S1). Essentially the same is found for [UO₂(H₂O)(MeCN)₅]²⁺: in the gas phase, water is expelled after about 1 ps (after lifting all constraints) affording **0**, whereas in solution, an acetonitrile ligand dissociates rapidly, after about 0.6 ps, affording **1** (Figure 1). In particular the findings for the latter system, [UO₂(H₂O)(MeCN)₅]²⁺, are noteworthy, because it shows a noticeable extent of “meta-stability”. All uranium-ligand bonds can undergo at least one full stretching vibration before the dissociation occurs (most bonds can undergo many more). The observed events are thus less likely to be biased by a particular starting configuration.

(36) We are not claiming that this particular mechanism for ligand exchange would be the most favorable one for the complexes under scrutiny. The limited statistical significance of the single events notwithstanding, we are probing the apparent driving forces for systems in this transient region of phase space.

In any event, these results are fully consistent with the static non-periodic DFT calculations discussed above. A quantitative assessment would be possible via constrained MD and pointwise thermodynamic integration, which has been shown to reproduce ligand binding energies in aqueous solution with reasonable accuracy.^{14–16} However, as the systems of this study require larger boxes and, thus, considerably more CPU time than the aqueous analogues, this technique was not applied.

The solvent distribution around **1** (obtained after acetonitrile elimination from [UO₂(H₂O)(MeCN)₅]²⁺ in solution) is assessed by way of radial distribution functions (RDFs) between the H atoms of the ligands and the N atoms of the solvent (Figure 2a). As is evident from the sharp maximum below 2 Å (solid red line in Figure 2),³⁷ the water ligand binds solvent molecules rather strongly. Integrating this first peak in the H(H₂O)–N RDF up to $r = 2.55$ Å indicates that each water H atom has on average 1.0 MeCN molecules attached to it. A representative snapshot from the CPMD simulation is shown in Figure 2b.

In contrast, there is a much weaker organization of the solvent around the methyl groups of the acetonitrile ligands (cf. the dashed blue line in Figure 2). Only a very shallow, rugged maximum is apparent at about 3 Å. The better solvation of the water ligand as compared to coordinated acetonitrile is also apparent in two representative microsolvated [UO₂(H₂O)(MeCN)₄]²⁺·2MeCN isomers (Figure 3). Isomer **1A**, which has the two extra solvent molecules bonded to the water ligand, is more stable by about 19 kcal/mol than isomer **1B**, in which the extra solvent molecules make contacts with the

(37) The second maximum in the solid red curve above 3 Å stems from the distances between one water H atom and an acetonitrile bound to the other H atom.

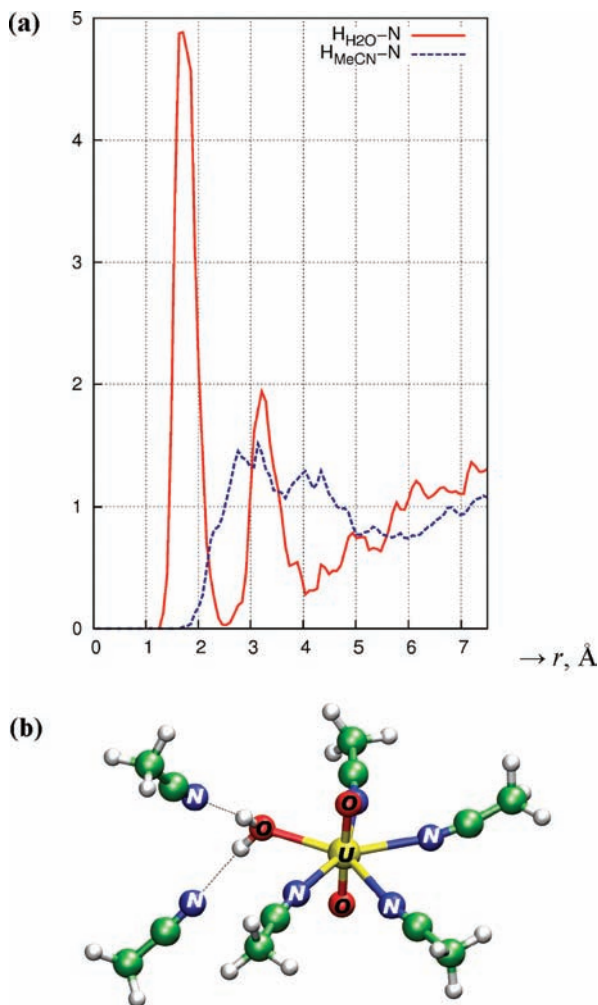


Figure 2. (a) Solvation of the H₂O and MeCN ligands of **1**. Radial distribution functions of N_{MeCN} around X (X = H₂O or H_{MeCN}; averages over the last 2 ps of MD). The four coordinated N atoms were not taken in account for the computation of the RDFs. (b) Snapshot of the [UO₂(H₂O)(MeCN)₄]²⁺ complex in solution after 3 ps of CPMD, illustrating the solvation mode of the aquo ligand, where each H atom is hydrogen-bonded to an acetonitrile solvent molecule. Other solvent molecules are hidden for clarity.

acetonitrile ligands.³⁸ In agreement with this energy difference, **1A** is stable in a CPMD simulation in the gas phase, while **1B** is not: the two extra MeCN molecules in the latter are so weakly bound that they dissociate spontaneously (within ca. 2 ps).

The geometry of the H₂O ligand in **1A** is particularly noteworthy: its O–H distance is about 0.03 Å longer than in the OH₂···(NCMe)₂ trimer or in pristine H₂O, while

(38) There are, arguably, many more possible isomers of **1B**; it is unlikely, however, that they will be similar or even lower in energy than **1A**. **1B** can be considered representative for the solvation of the acetonitrile ligands in the CPMD simulation of the actual solution inasmuch as the solvent molecules around these ligands are rather mobile and are frequently found in “bridging” positions similar to the “upper” red MeCN molecule in **1B** in Figure 3.

(39) Despite frequent claims that DFT would not be able to describe hydrogen bonding adequately, the accuracy of geometrical parameters and binding energies of H-bonded systems can be quite respectable: For example, for water clusters, the mean average errors in binding energies are below 1 and 0.5 kcal/mol with BLYP and B3LYP, respectively: Santra, B.; Michaelides, A.; Scheffler, M. *J. Chem. Phys.* **2007**, *127*, 184104, and for the HCNHF complex, a high-level coupled-cluster binding energy is reproduced within 0.5 kcal/mol with B3LYP. Domagala, M.; Grabowski, S. *J. Chem. Phys.* **2009**, *363*, 42–48.

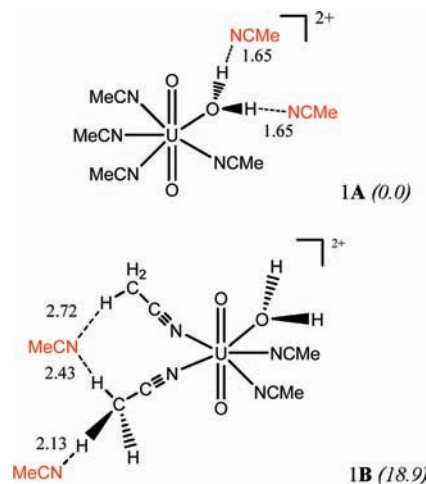


Figure 3. [UO₂(H₂O)(MeCN)₄]²⁺ complex **1** “solvated” by 2 MeCN molecules interacting with either H₂O (structure **1A**) or with MeCN ligands (structure **1B**), including typical H-bonded distances (in Å). In parentheses: relative gas-phase energies in kcal/mol, BLYP/SDD(+), single points on BLYP/SDD geometries.

its H–O–H angle opens to 108.5°, providing structural evidence for very strong hydrogen-bonding interactions with water.³⁹

3.4. Charge Distributions. The much stronger solvation of the aquo than the acetonitrile ligands and concomitant strengthening of the U–OH₂ bond appears to be one reason for the apparent stabilization of water ligands in solution. To get further insights into related electronic effects (mainly charge transfer and polarization), charge distributions were analyzed in terms of standard atomic populations analyses (Table 3) and localized Wannier functions (Table 4), focusing on complex **1**. In context with the very different energetics in the gas phase and a continuum (see Table 2), interesting differences in atomic charges are obtained in the two media, both with Mulliken and natural population analysis (NPA, Table 3). According to these analyses, significant charge transfer to the UO₂ moiety occurs ($q_{\text{UO}_2} \approx 0.6 e$ to $0.8 e$ rather than $+2 e$ in pristine UO₂²⁺). This transfer is larger (by up to 0.1 e) in solution than in the gas phase, indicative of a specific stabilization of the complex in solution. A similar trend is found for the homoleptic complexes **0** and **5** (results not shown). Furthermore, looking at the different ligand contributions, it appears that MeCN is more positively charged than H₂O in the gas phase, while the reverse is observed in solution. These features are found with both Mulliken and NPA charges and seem to be consistent with our finding that acetonitrile is a stronger ligand than water in the gas phase, but not in solution. Looking at changes that would reflect polarization effects within each ligand, however, no systematic trend is observed with both charge schemes. For instance, on going from pristine **1** to the microsolvated form **1A**, a certain increase in polarization of the water ligand is apparent in the Mulliken charges (namely, the increased negative charge on the O atom, from about $-0.5e$ to $-0.6e$), but not in those from NPA.

To study such polarization effects, we thus turned to a more sophisticated analysis based on localized orbitals in the form of Wannier functions. Assuming the electronic charge is concentrated in points located on the centers of

Table 3. Atomic Charges at the BLYP/SDD Level

	Mulliken			NPA		
	1	1	1·2MeCN (1A)	1	1	1·2MeCN (1A)
	gas	PCM	gas	gas	PCM	gas
U	1.61	1.62	1.58	1.40	1.34	1.36
UO ₂	0.78	0.71	0.72	0.69	0.59	0.63
O _(H₂O)	-0.53	-0.55	-0.62	-0.86	-0.85	-0.85
H _(H₂O) ^a	0.37	0.42	0.38	0.55	0.59	0.53
H ₂ O	0.21	0.28	0.14	0.25	0.33	0.21
MeCN(first) ^b	0.25	0.25	0.22	0.27	0.27	0.24
MeCN(second) ^c			0.13			0.10

^a Mean value for the two H_(H₂O) hydrogen atoms. ^b Mean sum over MeCN in first coordination shell (i.e., sums over single ligands, averaged over all ligands of the same kind). ^c Mean sum over MeCN in second solvation shell.

Table 4. Influence of the Environment on the Geometry and Dipole Moment of H₂O^a

species	H ₂ O geometry ^b		$\mu_{\text{H}_2\text{O}}$ (D)	
	<i>d</i> _{OH}	θ_{HOH}	complex ^c	isolated ^d
H ₂ O	0.977	104.2		1.84 [1.80]
OH ₂ ···(NCMe) ₂	0.981	102.9	2.26	1.86
[UO ₂ (H ₂ O)] ²⁺	0.993	106.9	5.05	1.80 [1.77]
[UO ₂ (H ₂ O)(MeCN)] ²⁺ ^e	0.988	106.7	4.48	1.82
[UO ₂ (H ₂ O)(MeCN) ₄] ²⁺ (1)	0.980	107.4	3.49 (3.44) ^f	1.78 [1.76]
[UO ₂ (H ₂ O)(MeCN) ₄] ²⁺ ·2MeCN (1A)	1.018	108.5	5.09 (4.78)	1.77

^a Obtained using Wannier-function centers; see text. ^b O–H distance (in Å) and H–O–H angle (in degrees). ^c Dipole moment (D in Debye) of H₂O within the complex (in parentheses: mean value over 50 snapshots taken over the last 1 ps of a CPMD simulation in the gas phase). ^d Dipole moment (D) of an isolated water molecule in the same geometry as in the complex [in brackets: true value computed from the electronic wave function]. ^e Linear MeCN–UO₂²⁺–OH₂ complex (transition state for N–U–O bending). ^f Dynamic average in acetonitrile solution: 4.45 D.

the Wannier functions (corresponding to electron pairs of bonds or lone pairs; see, for example, Supporting Information, Figure S6 and Table S5), dipole moments of fragments within a molecule or a periodic array of molecules can be calculated.⁴⁰ This approach has been used successfully to evaluate the dipole moments of individual water molecules in bulk water.⁴¹ Our calculated values for pristine H₂O and MeCN molecules (1.8 and 4.0 D, respectively) satisfactorily reproduce the corresponding experimental values (1.8 and 3.4 D). The results for **1** and related fragments or adducts are collected in Table 4.

Attachment of two acetonitrile H-bond acceptors to a water molecule significantly increases its dipole moment, both for a single water molecule (compare first two entries in Table 4) and for a water ligand in complex **1** (compare last two entries in Table 4). This polarization is not a geometrical effect (salient structural parameters are included in Table 4) and is not readily apparent in total atomic charges obtained from standard population analysis (e.g., for going from **1** to **1A**, Table 3). Coordination to uranyl also induces a strong polarization of the water ligand.

Similar values are obtained for static minima and the dynamic average over a CPMD trajectory (values in parentheses in Table 4). For the dynamic average for **1** in acetonitrile solution, a mean water dipole of 4.45 D is

obtained (standard deviation 0.35 D), much closer to that of **1A** (4.78 D) than to that of pristine **1** (3.44 D, Table 4).

Closer inspection of the positions of the Wannier centers (Supporting Information, Table S5) reveals that it is mainly the positions of the two lone pairs at the O_{H₂O} atom that are responsible for the increase of the dipole moment. For example, on going from gaseous **1** to **1A**, the angle X–O–X (where X denotes the “lone-pair” Wannier centers) closes from about 107° to about 95°.

A similar analysis is presented for selected acetonitrile moieties in Table 5. Polarization of this ligand upon coordination to the metal fragment is even larger than for water (compare the values for the isolated molecules and complexes **1** in Tables 4 and 5). A further slight increase of the dipole moment of an acetonitrile ligand upon coordination of two MeCN molecules in the second shell is found for the static minimum **1B** (from ca. 7.6 to 8.4 D). This seemingly enhanced polarization is not retained in the bulk solution, however: For the dynamic average for **1** in acetonitrile solution, a mean MeCN dipole of 7.33 D is obtained (standard deviation 0.50 D), essentially identical to the dynamic average for **1** in the gas phase, 7.36 D.

4. Discussion

Static DFT and CPMD results agree that in the gas phase, MeCN has a higher affinity toward uranyl than water. Because acetonitrile has a higher dipole moment than water ($\mu = 3.4$ and 1.8 D, respectively)⁴² and a higher polarizability than water ($\alpha = 4.4$ and 1.5 Å³, respectively)⁴² the gas phase results follow expected trends in charge-dipole and

(40) This procedure affords a very simple point-charge model, where the positive atomic charges (screened by the core if present) are placed at the nuclear positions, and negative charges of -2 at the positions of the Wannier centers. The total dipole moment is then calculated from this distribution of point charges.

(41) See: Silvestrelli, P. L.; Parrinello, M. *J. Chem. Phys.* **1999**, *111*, 3572–3580, and references cited herein.

(42) Marcus, Y. *Ion Solvation*; Wiley: Chichester, 1985.

Table 5. Influence of the Environment on the Dipole Moment of MeCN^a

species	$\mu_{\text{MeCN}} \text{ (D)}$		$\mu_{\text{OH}_2 \cdots (\text{NCMe})_2} \text{ (D)}^d$
	first shell ^b	second shell ^c	
MeCN	4.01		
$\text{OH}_2 \cdots (\text{NCMe})_2$		4.34	6.15 [6.16]
$[\text{UO}_2(\text{H}_2\text{O})(\text{MeCN})]^{2+ e}$	10.48		
$[\text{UO}_2(\text{H}_2\text{O})(\text{MeCN})_4]^{2+ (1)}$	7.62 (7.36) ^f		
$[\text{UO}_2(\text{H}_2\text{O})(\text{MeCN})_4]^{2+} \cdot 2\text{MeCN (1A)}$	7.06 (6.87) ^{f,g}	6.21 (5.66) ^f	13.33
$[\text{UO}_2(\text{H}_2\text{O})(\text{MeCN})_4]^{2+} \cdot 2\text{MeCN (1B)}$	8.44 ^h	5.43	

^a Obtained using Wannier-function centers (see text). ^b Free MeCN or MeCN coordinated to uranyl. ^c MeCN coordinated to H₂O. ^d OH₂⋯(NCMe)₂ fragment [in brackets: true value computed from the electronic wave function]. ^e Linear MeCN–UO₂²⁺–OH₂ complex (transition state for N–U–O bending). ^f In parentheses: mean value over 50 snapshots taken over the last 1 ps of a CPMD simulation in the gas phase. ^g Dynamic average in acetonitrile solution: 7.33 D. ^h Dipole of the solvated MeCN ligand.

charge-induced dipole interactions with the uranyl cation. As noticed above and by other related studies,⁴³ charge transfer and polarization effects also contribute to the stronger affinity of uranyl for acetonitrile over water. Our results agree with recent gas-phase DFT results¹⁷ and with experiments using electrospray ionization, ion-cyclotron resonance, and infrared multiphoton dissociation techniques, where attempts to generate pristine $[\text{UO}_2(\text{H}_2\text{O})_n]^{2+}$ species in the gas phase were unsuccessful,⁴⁴ whereas $[\text{UO}_2(\text{MeCN})_n]^{2+}$ species up to $n = 5$ (i.e., complex **0**) were readily formed.⁴⁵ While the latter complexes were found to add either water or additional acetonitrile ligands up to a total coordination number of five, complex **0** did not react with additional water, that is, water does not displace acetonitrile in the gas phase.⁴⁶ In “humid” acetonitrile solution, however, we calculate that uranyl prefers water over acetonitrile, because of specific synergistic features: (i) the UO₂(OH₂) moiety is much better solvated by acetonitrile than the UO₂(NCMe) moiety, and (ii) the U–OH₂ bond is reinforced by solvation, while the U–NCMe bond is little affected. In the following, we discuss related structural and electronic effects.

Structural Features. The U–N bond distance is remarkably insensitive to the surrounding: most optimized or MD-averaged bond lengths are between 2.53 and 2.58 Å (Table 1). This range compares well to EXAFS data for **0**, 2.53 Å,⁵ and to the mean U–N distance of 2.56 Å found for uranyl-acetonitrile complexes in the solid state.⁴⁷ In contrast, U–O_{eq} distances to the water ligands decrease considerably on going from the gas phase to the bulk, by up to 0.15 Å (Table 1). Similar trends were observed for uranyl-aquo complexes in aqueous solution. Actually, the same U–O_{eq} distance of 2.47(9) Å is obtained from CPMD simulations of the pentaquo complex **5** both in water¹¹ and in acetonitrile (Table 1).

For the water ligand, the observed bond contraction upon solvation correlates with the computed increase in bond strength. According to the PCM results, this reinforcement is enough to switch the relative affinity of both ligands on going from the gas phase into the bulk (Table 2).⁴⁸ Thus, in solution, uranyl should preferentially bind water rather than acetonitrile ligands. Even though less conclusive in a quantitative sense, this different relative affinity is corroborated by CPMD simulations of six-coordinated mixed uranyl-water-acetonitrile complexes, $[\text{UO}_2(\text{H}_2\text{O})_3(\text{MeCN})_3]^{2+}$ and $[\text{UO}_2(\text{H}_2\text{O})(\text{MeCN})_5]^{2+}$, which were found to spontaneously lose a water and an acetonitrile ligand in the gas phase and in solution, respectively (Figure 1 and Supporting Information, Figure S1).

These results are in complete agreement with a recent EXAFS study of uranyl chloro complexes in acetonitrile, which were prepared from UO₂(ClO₄)₂·6H₂O and NBu₄Cl salts.⁵ With the pure uranyl precursor, no evidence for species with U–N bonds could be found, and all uranium appeared to be present in the form of **5**. Thus, even though the solvent is present in a large excess (at uranyl concentrations of 50 mM), it does not displace the few H₂O ligands coming from the crystal water. Only with higher chloride concentrations mixed chloro-aquo-acetonitrile complexes were detected, from which the data for **0** in Table 2 were extrapolated.

Solvation and Ligand Polarization. In the CPMD simulations of **1**, **3**, and **5** in acetonitrile, strong persistent O–H⋯N hydrogen bonds between the water ligands and acetonitrile molecules from the solvent were apparent, with no exchange between these H-bound acetonitrile molecules and solvent from the bulk during the few picoseconds of our simulation. For instance, each water H atom in solvated **1** binds about 1.0 solvent molecules on average, with a mean H⋯N distance less than 2 Å (see Figure 2). Essentially the same is found for an acetonitrile solution of **3** and **5** (see RDFs in Supporting Information, Figure S4). Similar persistent O–H⋯O hydrogen bonds had been found in CPMD simulations of aqueous **5**.¹¹ According to the analysis of the localized Wannier centers, such hydrogen-bonding to acetonitrile affects the positions of these centers such that an increase of the dipole moment

(43) The importance of polarization effects on the energy profile of uranyl-water dissociation has been noted previously: Hemmingsen, L.; Amara, P.; Ansoborlo, E.; Field, M. J. *J. Phys. Chem. A* **2000**, *104*, 4095–4101.

(44) These species always contained additional, coordinated anions (such as nitrate or perchlorate from the stock solutions); see, for example, Anbalagan, V.; Chien, W.; Gresham, G. L.; Groenewold, G. S.; Van Stipdonk, M. J. *Rapid Commun. Mass. Spectrom.* **2004**, *18*, 3028–3034.

(45) Groenewold, G. S.; et al. *J. Am. Chem. Soc.* **2006**, *128*, 4802–4813.

(46) Van Stipdonk, M. J.; Chien, W.; Bulleigh, K.; Wu, Q.; Groenewold, G. S. *J. Phys. Chem. A* **2006**, *110*, 959–970.

(47) Five mononuclear UO₂-NCMe fragments with U–N distances between 2.51 Å and 2.61 Å were found in the Cambridge Structure Database: (a) Hall, T. J.; et al. *J. Crystallogr. Spectrosc. Res.* **1989**, *19*, 499. (b) Cametti, M.; et al. *J. Am. Chem. Soc.* **2007**, *129*, 3641, refocodes HEYYAM, SAZDOM, YALSAG, YALSOU.

(48) For more accurate PCM results, the second solvation shell may have to be included explicitly, cf. the situation in aqueous uranyl hydrate: (a) Shamov, G. A.; Schreckenbach, G. *J. Phys. Chem. A* **2005**, *109*, 10961–10974. (b) Shamov, G. A.; Schreckenbach, G. *J. Phys. Chem. A* **2006**, *110*, 12072.

of the water molecule ensues (Table 4). This effect is found already in an isolated water molecule (where binding of two acetonitrile molecules increases the water dipole moment (1.87 D) roughly to that of a water molecule in the water dimer (2.15 D using the same methodology).⁴¹ The concomitant increase in the dipole moment upon solvation is even more pronounced for a uranyl-complexed water molecule,⁴³ for example, from about 3.5 D to about 5 D on going from **1** to **1A** (Table 4). Arguably, this gain in dipole moment is the main reason for the increased binding energy and decreased U–O distance of a water ligand in solution.⁴⁹

The second solvation shell thus exerts a strong polarization of the water ligands in the first shell. This polarization does not manifest itself in a charge shift between atoms, so that atomic charges from standard population analyses are not affected much.⁵⁰ Rather, positions of the charge densities (notably those of the formal lone pairs on oxygen) are shifted within the atomic basins, resulting in a net increase of the dipole moment of the water molecules. That this increase is more pronounced for a uranyl-complexed water ligand than for a free water molecule (Table 4) is a clear indication of cooperativity. Facilitated by such cooperative polarization, the ditopic coordination $M^{n+} \cdots OH_2 \cdots A$ (M = metal, A = H-bond acceptor) is much more favorable than a similar $M^{n+} \cdots NC-CH_3 \cdots A$ arrangement (cf. the large energetic difference between microsolvated isomers with these structural motifs, Figure 3). The ubiquity of the former and the much lower abundance of the latter fragments in solid-state structures support this interpretation.⁵¹ Evidently, these observations are directly linked to the $C-H \cdots X$ hydrogen-bond strengths, which are much lower than those of their $O-H \cdots X$ counterparts.^{52,53}

As mentioned above, acetonitrile itself has a higher permanent dipole moment and a higher polarizability than water and, accordingly, its dipole moment increases significantly upon complexation to uranyl (e.g., from about 4 D in free MeCN to 7.6 D in **1**, see static values in Table 5). However, because of the lack of strong cooperativity effects, this value is not enhanced further in solution (cf. 7.4 and 7.3 D in gaseous and solvated **1**, respectively, CPMD-averaged values). The absolute values of the ligand dipole moments do thus not give a sufficient indication for the stability of a particular complex in a given environment. The gas-to-liquid trends, however, help to rationalize why water is a better ligand in solution than in the gas phase. In this context it is also interesting to note that the $OH_2(NCMe)_2$ unit itself, that is, a water molecule with two H-bonded acetonitrile molecules, has a higher dipole moment than each of its

constituents, and that this dipole moment is massively enlarged by coordination to uranyl (see the last column in Table 5).

The nature of the bonding of acetonitrile to uranyl has been studied before. While electron donation from the N lone pair to uranyl has been inferred from Kohn–Sham molecular orbitals,⁵⁴ charge decomposition analysis has indicated predominantly ionic bonding.⁴⁵ Our analysis of the dipole moments would be consistent with such a significant ionic part in the bonding.

Our findings may have implications beyond the special case of uranyl salts in water and acetonitrile. Cooperative polarization effects may also explain why, for instance, K^+ and Cl^- ions individually interact more strongly with MeCN than with H_2O in the gas phase, while the KCl salt prefers water over acetonitrile solution (ΔG for the transfer from water to acetonitrile amounts to +12 kcal/mol).⁵⁵ In lanthanide chemistry, it has long been known that the affinity of lanthanide ions Ln^{3+} toward water is much higher than toward acetonitrile in mixtures of the two solvents, for example, for $Ln = Eu$.⁵⁶ Also, lanthanide salts containing $[Ln(NCMe)_n]^{3+}$ ions ($n = 8, 9$; $Ln = Nd, Eu, Gd, Dy, Tm$) have been described as hygroscopic requiring rigorous exclusion of water,⁵⁷ consistent with a propensity of the latter for replacing the acetonitrile ligands. This propensity is corroborated by preliminary calculations at the B3LYP/pVTZ level, according to which the displacement of the water ligands in $[La(H_2O)_9]^{3+}$ by nine acetonitrile ligands is indeed favorable in the gas phase, but unfavorable in the continuum.⁵⁸

Similar effects are to be expected for other solvents that are more polar and polarizable than water but that are less likely to be prone to cooperative polarization by the second solvation shell (e.g., DMSO, amides, ketones, phosphoryl groups). Cooperative polarization effects have been described in host–guest chemistry⁵⁹ and have been suggested to be important for the properties of solid and liquid water itself.⁶⁰ That these effects may also underpin parts of standard coordination chemistry has, to our knowledge, not been emphasized before.

An alternative view of the water preference over acetonitrile in solution is that $M(H_2O)_x^{n+}$ complexes are much better solvated than $M(MeCN)_x^{n+}$ analogues, because (i) they are smaller in size and, according to the simple Born solvation model,⁶¹ the free energy of solvation varies with $1/R$, where R is the effective radius of the corresponding spherical cavity; (ii) they form much stronger hydrogen bonds with the solvent. However, as discussed above, further stabilization of the complex itself (by increased charge transfer and polarization effects) also markedly contributes to the hygroscopic character of $M(MeCN)_x^{n+}$ complexes in condensed phases.

(49) Attraction between the uranyl moiety and second-shell solvent molecules further compresses the first solvation shell (“constriction effect”).

(50) Atoms-in-Molecules analyses of water clusters, on the other hand, have indicated charge transfer between atoms as origin of polarization: Devereux, M.; Popelier, P. L. A. *J. Phys. Chem. A* **2007**, *111*, 1536–1544.

(51) A search for M–OH₂ and M–N≡C–CH₃ fragments in the Cambridge Structure Database with any other atom approaching hydrogen to within the sum of van-der-Waals radii returns ca. 16,400 and 3000 hits, respectively.

(52) See, for instance: Gu, Y.; Kar, T.; Scheiner, S. *J. Am. Chem. Soc.* **1999**, *121*, 9411–9422.

(53) Despite their relative weakness, the importance of C–H⋯X interactions for determining crystal structures is well recognized; see, for example, Biradha, K. *CrystEngComm* **2003**, *5*, 374–384.

(54) Schoendorff, G.; Windus, T. L.; de Jond, W. A. *J. Phys. Chem. A* **2009**, *113*, 12525–12531.

(55) Cox, B. G. *Chem. Soc. Rev.* **1980**, *9*, 381.

(56) Haas, Y.; Stein, G. *J. Phys. Chem.* **1971**, *75*, 3677–3681.

(57) Bodizs, G.; Raabe, I.; Scopelliti, R.; Krossing, I.; Helm, L. *Dalton Trans.* **2009**, 5137–5147.

(58) A full account of these computations will be published separately.

(59) For example, (a) Hughes, M. P.; Smith, B. D. *J. Org. Chem.* **1997**, *62*, 4492–4499. (b) Cooke, G.; Rotello, V. M. *Chem. Soc. Rev.* **2002**, *31*, 275–286.

(60) For example, (a) Heggie, M. I.; Latham, C. D.; Maynard, S. C. P.; Jones, R. *Chem. Phys. Lett.* **1996**, *249*, 485–490. (b) Stokeley, K.; Mazza, M. G.; Stanley, H. E.; Franzese, G. *Proc. Nat. Acad. Sci.* **2010**, *107*, 1301–1306.

(61) Born, M. *Z. Physik* **1920**, *1*, 45–48.

On the methodological side, what is remarkable is that a simple continuum model can reproduce the solvation effects so well, in particular the reinforcement of the U-water bonds in solution. Similar bond contractions upon immersion in a continuum have been found for main-group aquo ions, but only if a molecule-shaped cavity is used (as in our PCM calculations).⁶² Applying the simple PCM approach to model the water/acetonitrile competitive binding to trivalent lanthanides, we indeed predict, as for uranyl, that MeCN is a stronger ligand in the gas phase, whereas H₂O is preferred in solution.⁵⁸

5. Conclusion

We have presented the first CPMD simulation of uranyl complexes in a non-aqueous solvent, acetonitrile. In conjunction with BLYP and B3LYP optimizations in a polarizable continuum modeling of this solvent, water ligands are found to have a lower affinity for uranyl than acetonitrile in the gas phase, whereas the relative binding strengths are reversed in acetonitrile solution. The uranium-water bonds are particularly strongly reinforced upon solvation, which is reflected in a significant U–O bond contraction. Using a simple point-

charge model from localized orbitals, this effect can be traced back to an increased polarization of the water ligand in solution. Through rather strong O–H···N hydrogen bonds, the acetonitrile molecules in the second solvation shell increase the dipole moment of the water ligand substantially, thus forming stronger hydrogen bonds. This cooperative polarization of water in a metal-water-acceptor array reinforces the ionic part of the metal-water bond. Acetonitrile is intrinsically (i.e., in the gas phase) a better ligand than water, but cannot profit from an analogous increase in polarity because it exerts only weak specific interactions toward the surrounding solvent. Beyond the uranyl case, this study points to the importance of cooperative polarization effects to enhance the Mⁿ⁺ ion affinity for water in condensed phases involving Mⁿ⁺–OH₂···A fragments, where A is a H-bond proton acceptor and Mⁿ⁺ is a hard cation.

Acknowledgment. This work was supported by EaStChem via the EaStChem Research Computing facility and a local Opteron PC cluster maintained by Dr. H. Früchtl. A.C. and W.G. are grateful to IDRIS, CINES, the Université de Strasbourg, as well as GDR CNRS PARIS for computer resources.

Supporting Information Available: Additional computational details, graphical and tabular material, full citations of ref 29 as well as optimized coordinates of **0** to **5**. This material is available free of charge via the Internet at <http://pubs.acs.org>.

(62) A spherical cavity as in the simple Kirkwood–Onsager model results in a bond elongation in the continuum; see, for example, Martinez, J. M. M.; Pappalardo, R. R.; Marcos, E. S.; Mennucci, B.; Tomasi, J. *J. Phys. Chem. B* **2002**, *106*, 1118–1123.